7722 *Biochemistry* **2009,** *48,* 7722–7731
DOI: 10.1021/bi900516n

BIOCHEMISTRY
including biophysical chemistry & molecular biology
Article

Impact of Cardiac Troponin T N-Terminal Deletion and Phosphorylation on Myofilament Function[†]

Marius P. Sumandea,*[,‡] Susan Vahebi,[§] C. Amelia Sumandea,[‡] Mary L. Garcia-Cazarin,[‡] Jon Staidle,[∥] and Earl Homsher[∥]

[‡]*Department of Physiology, University of Kentucky, Lexington, Kentucky 40536,* [§]*Department of Physiology and Biophysics, University of Illinois at Chicago, Chicago, Illinois 60612, and* [∥]*Department of Physiology, University of California Los Angeles, Los Angeles, California 90095*

Received April 10, 2009; Revised Manuscript Received July 6, 2009

ABSTRACT: Cardiac troponin T (cTnT) is a phosphoprotein that modulates cardiac muscle contraction through its extensive and diverse interactions with neighboring thin filament proteins. Its N-terminal half is the "glue" that anchors the troponin complex to tropomyosin−actin. Until now, studies aimed at investigating the role of the N-terminal tail region have not considered the effects of phosphorylation. To understand better the regulatory role of the N-terminal tail region of phosphorylated cTnT, we investigated the functional effects of N-terminal deletion (amino acids 1−91) and phosphorylation on Ca^{2+} dependence of myofilament isometric force production, isometric ATPase rate, and thin filament sliding speed. Chemomechanical profiles were assessed in detergent permeabilized fiber preparations where the native troponin (cTn) was exchanged with recombinant cTn engineered to contain modified cTnT (truncated, phosphorylated) in the presence of wild-type cTnI and cTnC. Removal of the cTnT N-terminal amino acids 1−91 (cTnT-del) enhances myofilament responsiveness to nonsaturating Ca^{2+} levels (the physiological range in cardiac myocytes). However, at saturating Ca^{2+} levels, there is a reduction in isometric tension and ATPase rate. On one hand, phosphorylation of cTnT-del attenuates the sensitizing effect induced by truncation of the N-terminal tail, "resetting" myofilament Ca^{2+} responsiveness back to control levels. On the other hand, it impairs isometric tension development and ATPase rate. Interestingly, phosphorylation of cTnT (cTnT-P) differentially regulates tension cost (an index of cross-bridge cycling rate): increased by cTn-del-P and decreased by intact cTn-wt-P. Like the isometric fiber data, sliding speed of thin filaments regulated by cTn-del is more sensitive to Ca^{2+} compared with cTn-wt. Phosphorylation of cTnT (whether cTnT-del or -wt) depresses sliding speed and is associated with Ca^{2+} desensitization of thin filament sliding speed.

In recent years numerous studies have provided strong support for the hypothesis that phosphorylation of thin filament proteins is a key modulator of cardiac function (*1*, *2*). Phosphorylation of cardiac troponin T (cTnT)[1] produces significant functional effects (*3*, *4*) by its diverse interactions with other troponin subunits, tropomyosin, and actin. cTnT is considered the "lever" on the thin filament that transmits the signal generated by Ca^{2+}-induced conformational changes in cardiac troponin C (cTnC) and cardiac troponin I (cTnI) to the filamentous protein tropomyosin (Tm). Upon Ca^{2+} activation, Tm moves over the actin filament surface to promote cross-bridge binding to the thin filament and initiate contraction (*5*, *6*).

Tethering of the heterotrimeric troponin complex to the thin filament is largely mediated by the N-terminal portion of cTnT, which interacts with and influences the Tm-Tm end-to-end interaction region. In addition to its critical function anchoring tropomyosin to actin, the N-terminal region may also have inhibitory effects on myosin interaction with the thin filament (*7*, *8*). The N-terminal tail region of cTnT is particularly important because it gives functional diversity to cardiac myofilaments through alternative splicing that may have developmental specific roles (*4*). Switches in the cTnT isoform expression have been implicated in diabetes, cardiac hypertrophy, and congenital heart disease (*9*). The essential role of the N-terminal tail was accentuated by the discovery of charge mutations in this region that cause familial hypertrophic cardiomyopathy (*10*, *11*). However, until now, studies aimed at investigating the role of the N-terminal region have not considered the effects of phosphorylation (*12*−*14*), although cTnT is phosphorylated even in resting cardiomyocytes.

cTnT is phosphorylated by a variety of Ser/Thr kinases such as the protein kinase C (PKC) family at Thr^{197}, Ser^{201}, Thr^{206}, and Thr^{287} (*15*−*17*), Rho-A-dependent protein kinase (ROCK-II) at Ser^{278} and Thr^{287} (*18*), apoptosis signal-regulating kinase (ASK-1) at Thr^{197} and Ser^{201} (*19*), and Raf-1 at Thr^{206} (*20*). PKC-dependent phosphorylation of cTnT is thought to be important in the development of cardiac hypertrophy/failure syndromes. cTnT phosphorylation has been shown to depress contractile function (*15*, *18*). This effect was associated with desensitization of the myofilament response to Ca^{2+} and a decrease in cross-bridge cycling rate (tension cost) (*15*).

To understand better the regulatory role of the N-terminal region of a phosphorylated cTnT, we investigated the functional effects of N-terminal deletion (amino acids 1−91) and phosphorylation on Ca^{2+} dependence of myofilament force production, ATPase rate, and thin filament sliding speed.

[†]This work was supported by grants from NIH-NIA AG032009 and AHA-SDG 0335199N (M.P.S.) and by USPHS Grant AR30988 (E.H.).

*Address correspondence to this author. Tel: 859-323-6613. Fax: 859-257-2896. E-mail: MariusSumandea@uky.edu.

[1]Abbreviations: cTnT, cardiac troponin T; cTnI, cardiac troponin I; cTnC, cardiac troponin C; cTnT-del, cardiac troponin T lacking amino acids 1−91; cTnT-P, phosphorylated cTnT; cTnT-del-P, phosphorylated cTnT-del; cTn, cardiac troponin complex; Tm, tropomyosin; PKC, protein kinase C.

 Published on Web 07/08/2009

EXPERIMENTAL PROCEDURES

Generation of the cTnT-del Construct. A bacterial expression vector encoding the cDNA of cTnT-del (the truncated form of cTnT lacking N-terminal amino acids 1−91) was generated by polymerase chain reaction (PCR) using the pSBETa-cTnT plasmid as template (*15*). The following primers (from Operon) were used to produce cTnT-del: 5′-g aga gtg gac cat atg atg gac atc cac agg aag cgc gtg gag-3′ and 5′-gtt agc agc cgg atc ctg tga gcc agg gca g-3′ (underlined residues indicate the position of *Nde*I and *Bam*HI restriction endonuclease sites, respectively). The PCR product was then subcloned between the *Nde*I and *Bam*HI sites of the pSBETa vector. Construct identity was verified by DNA sequencing.

Troponin Expression and Purification. Recombinant mouse cardiac cTnT, cTnI, and cTnC were expressed and purified as previously described (*15*, *21*). Mouse cardiac cTnT-del was expressed and purified by a modified method of Sumandea et al. (*15*). Briefly, cTnT-del was expressed in BL21-(DE3) cells using the pSBETa expression plasmid. BL21(DE3) cells grown overnight in Luria broth supplemented with 30 μg/mL kanamycin were collected by centrifugation at 6000*g* for 10 min at 4 °C. The cell pellet was washed once in STE buffer (5% sucrose, 25 mM Tris-HCl, pH 8.0, 5 mM EDTA) and resuspended in sonication buffer (20 mM Tris-HCl, pH 8.0, 6 M urea, 5 mM EDTA, 0.1 mM aminoethylbenzenesulfonyl fluoride hydrochloride (AEBSF), 1 mM benzamidine, 1 mM DTT, and 0.5% Triton X-100). The cells were lysed by sonication on ice, followed by 60 min of centrifugation at 48000*g*, at 4 °C. The supernatant fraction was subjected to ammonium sulfate fractionation as previously reported (*22*). The final ammonium sulfate pellet was solubilized in buffer A (20 mM Tris-HCl, pH 8.0, 6 M urea, 1 mM EDTA) and then dialyzed at 4 °C against same buffer. The dialyzed sample was applied onto a SP-Sepharose column connected to an AKTA-FPLC system (GE Healthcare). cTnT-del was eluted with a 0.0−0.5 M NaCl gradient in buffer A. Fractions containing cTnT-del were analyzed by SDS−PAGE, and those >90% pure cTnT-del were pooled, extensively dialyzed against 0.05% TFA in H_2O, lyophilized, and stored in powder form at −80 °C.

cTnT Phosphorylation and Troponin Complex Reconstitution. cTnT-wt and cTnT-del were phosphorylated using recombinant human PKC-α (expressed in Sf9 cells) as previously described (*15*). cTnT-wt and cTnT-del (phosphorylated or unphosphorylated) were denatured and mixed with equimolar amounts of cTnI and cTnC followed by dialysis and ion-exchange chromatography to reconstitute and purify the trimeric troponin (cTn) complex (*15*). The cTn complex identity and purity were verified by SDS−PAGE.

MALDI-TOF Mass Spectrometry. cTnT-wt (or cTn-wt complexes for comparison) phosphorylated by recombinant human PKC-α (as above) or nonphosphorylated was digested with endoproteinase Glu-C from *Staphylococcus aureus* V8 (Roche). Phosphopeptides were enriched on gallium(III)-chelated IDA-based resin (Pierce). Matrix-assisted laser desorption/ionization time-of-flight (MALDI-TOF) analysis was performed as previously described (*23*, *24*).

Anti-cTnT Phospho-Specific pThr^{206} and pSer^{278} Antibody Production and Purification. Individual synthetic phosphopeptides, derived from the regions of the mouse cTnT sequence that contain Thr^{206} and Ser^{278}, were coupled to the keyhole limpet hemacyanin (KLH) carrier protein through a C-terminal Cys residue. Two rabbits were immunized per antibody (BioSource). Antibodies were purified from serum using sequential epitope-specific chromatography. Briefly, the antibody from the serum was first negatively preadsorbed onto a nonphosphorylated peptide affinity column to remove all antibodies that react with nonphosphorylated cTnT peptides. The product was then adsorbed twice onto a matrix containing immobilized phosphopeptide immunogen. The antibody bound and eluted from the final affinity column was then tested for phospho specificity, aliquoted, and stored at −80 °C.

Peptide Competition Assay. The specificity of anti-pThr^{206} and anti-pSer^{278} phospho antibodies was verified using a peptide competition assay. Briefly, a 200-fold molar excess of the phosphorylated peptide (used as immunogen for antibody production) and the corresponding nonphosphorylated peptide were preincubated with aliquots of the antibody for 30 min prior to addition to PVDF strips containing transferred proteins (see Figure 7 legend for more details). Reactivity of the antibodies with the membrane was detected by chemiluminescence using the ECL-plus kit (GE Healthcare).

Substitution of Native cTn by Recombinant cTn in Papillary Muscle Fiber Bundles. Fiber bundles were prepared from hearts of 5−6 month-old FVBN mice purchased from Harlan or Charles River Laboratories. Hearts were quickly removed under deep anesthesia (sodium pentobarbital; 100 mg/kg i.p.) and rinsed free of blood in ice-cold saline (0.9% NaCl). Muscle strips (∼150−200 μm wide and 3−4 mm long) were dissected from left ventricular papillary muscle. Fiber bundles were then detergent treated at 4 °C in a high relax buffer containing 20 mM MOPS, pH 7.0, 50 mM potassium propionate, 6.8 mM $MgCl_2$, 10 mM EGTA, 25 μM $CaCl_2$, 12 mM phosphocreatine, 5 mM Na_2ATP, 10 UI/mL creatine kinase, 0.5 mM DTT, a cocktail of protease inhibitors, and 1% Triton X-100 (*25*). Following the detergent treatment the fiber bundles were transferred to a bath containing a recombinant cTn complex (20−30 μM) in exchange buffer (20 mM MOPS, pH 6.5, 190 mM KCl, 5 mM EGTA, 5 mM $MgCl_2$, 1 mM DTT) and incubated overnight at 4 °C. The extent of native cTn substitution by recombinant cTn was determined after isometric tension and actomyosin Mg-ATPase activity measurements (see below) by immunoblot analysis of control vs exchanged fiber bundles, as previously described (*15*, *26*−*28*).

Mechanoenergetic Measurements. We measured isometric tension (force/cross-sectional area) and actomyosin Mg-ATPase activity simultaneously as described previously (*15*, *25*, *29*). Briefly, fiber bundles (control or exchanged) were attached to a displacement generator at one end and a force transducer at the other end using aluminum T-clips. Sarcomere length was adjusted to 2.3 μm using a laser diffraction pattern, and the cross-sectional area was determined based on an elliptical model. Fiber bundles were equilibrated for 5 min in relaxing buffer followed by 3 min in preactivating and then activating solutions. The composition of all buffers was described previously (*15*). Only those fibers able to generate >85% of the initial tension in their final contraction were analyzed. Isometric tension and actomyosin Mg-ATPase activity were determined simultaneously at 20 °C in the presence of variable Ca^{2+} concentrations as described (*15*). Data were analyzed using Labview (National Instruments, Austin, TX). The calcium dependence of the isometric tension is largely controlled by the rate at which cross-bridges enter into the isometric force bearing state while the rate at which the isometrically attached force bearing cross-bridges detach from

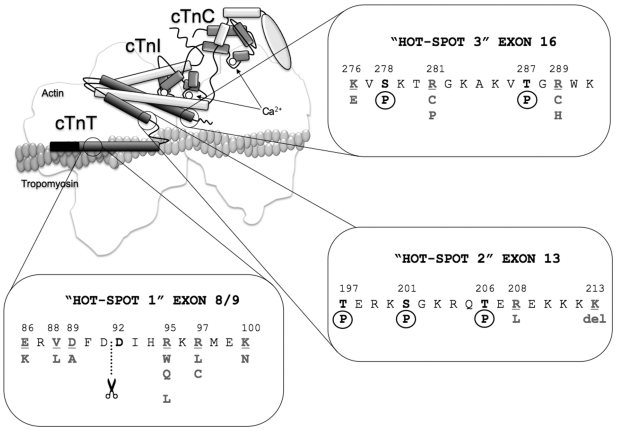

FIGURE 1: Schematic illustration showing the location of three functionally critical regions in cTnT. The drawing of the troponin complex is based on the crystal structure of the troponin core domain determined by Takeda et al. (*44*). The N-terminal region of cTnT (residues 1−204) was not solved in the crystal structure; therefore, our representation of this region is completely speculative. Rectangles represent helical structures. cTnC is colored light gray, cTnI is in white, and cTnT is in dark gray. The locations of three functionally critical regions or "hot spots" in cTnT are depicted (mouse sequence is used; it differs by three amino acids from the human counterpart). Some of the most severe cardiomyopathy-causing mutations are condensed in the three distinct regions. The region removed in this study, amino acids 1−91, is indicated. The N-terminal hypervariable region of cTnT (amino acids 1−71) is shown as a black rectangle. Deletion and missense mutations are shown in gray (original cTnT residues are underlined). P indicates phosphorylated residues.

the thin filament is minimally affected by the calcium concentration (*30*). Tension− and actomyosin MgATPase activity−[Ca^{2+}] relations were fit by a nonlinear fit procedure to a modified Hill equation as described (*15*).

In Vitro Motility Assay. Rhodamine phalloidin-labeled actin movement over heavy meromyosin-covered nitrocellulose surfaces was monitored in motility chambers by video epifluorescence microscopy and analyzed as previously described (*21*, *31*). Briefly, a rabbit skeletal heavy meromyosin solution (300 μg/mL) was injected into the motility chamber and allowed to incubate for 2 min. This was followed by 1 min incubation with 50 μL of 1 mg/mL bovine serum albumin in assay buffer (25 mM KCl, 25 mM MOPS, 2.0 mM EGTA, 2 mM $MgCl_2$, 5 mM DTT, pH 7.4). Next, 50 μL of 20 nM rhodamine phalloidin-labeled actin was introduced into the motility chamber and allowed to incubate for 2 min. The motility chamber was then washed with two 50 μL aliquots of assay buffer to remove unbound actin. This was followed by injection of 40 μL of a 50 mM ionic strength reconstitution solution containing regulatory proteins cTn (wt and del) and Tm, at 200 nM concentrations. The reconstitution solution consisted of 25 mM MOPS, 25 mM KCl, 2 mM $MgCl_2$, 2 mM EGTA (with varying ratios of CaKEGTA to K_2EGTA depending on the desired Ca^{2+} concentration), and 20 mM DTT. The chamber was incubated in this solution for 5 min, and the solution was replaced by two 40 μL washes of motility solution, which was a reconstitution solution to which 1 mM Na_2ATP and a glucose/oxidase/catalase mixture had been added to slow photobleaching (3 mg/mL glucose, 100 μg/mL glucose oxidase, 10 μg/mL catalase). Data were acquired and analyzed as previously described (*21*, *31*). The unloaded thin filament sliding speed is analogous to the unloaded shortening velocity in myocytes (*5*). As such, it is regulated primarily by the rate at which the strongly attached cross-bridges in the negative force bearing

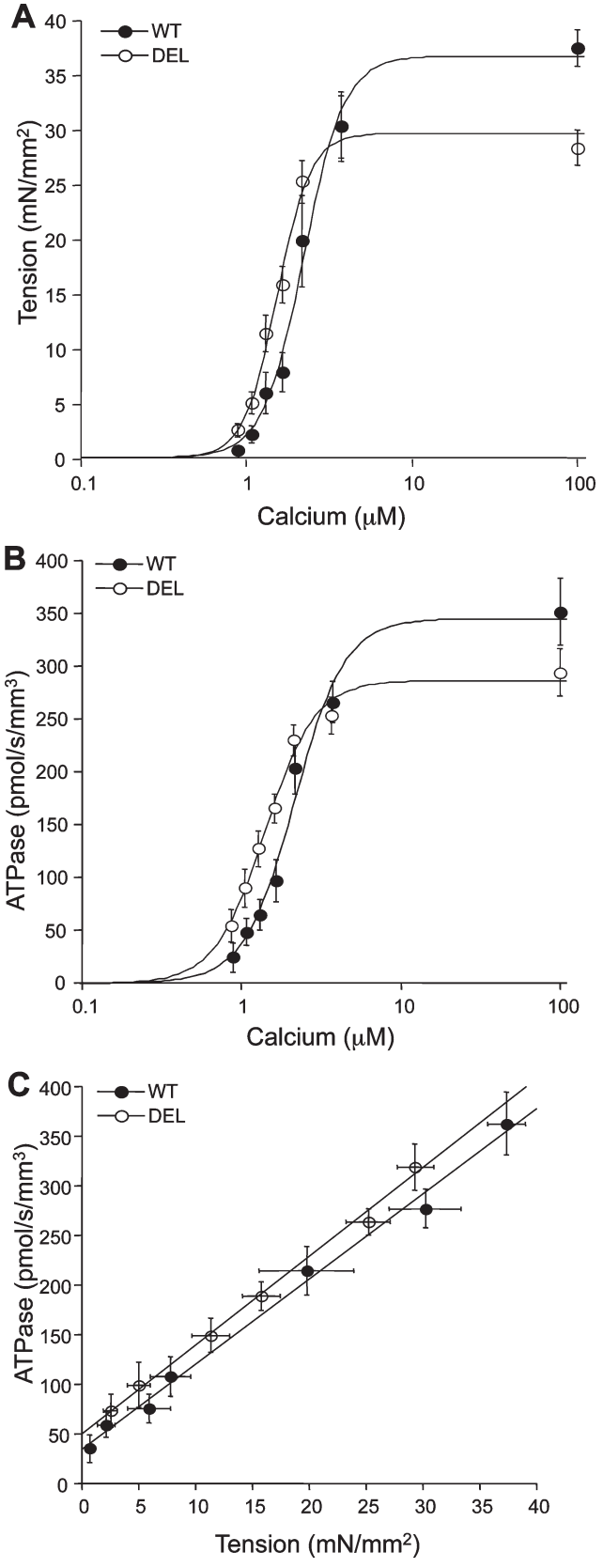

FIGURE 2: Mechanical characteristics of skinned fiber bundles exchanged with either cTn-wt or cTn-del (recombinant cTn complex containing cTnT-del, cTnI-wt, and cTnC-wt). Steady-state isometric tension (A) and actomyosin Mg-ATPase activity (B) were determined simultaneously at various [Ca^{2+}]. Tension cost (C) was determined from the slope of the relationship between actomyosin Mg-ATPase activity and isometric tension. Data are given as means ± SEM for $n = 9$ fiber bundles from seven separate hearts.

Table 1: Mechanical Profiles of Left Ventricular Papillary Fiber Bundles[a]

	Isometric Tension			ATPase				
TnT	Maximum (mN/mm^2)	EC_{50} (μM)	n_H (Hill coeff)	Maximum (pmol s^{-1} mm^{-3})	EC_{50} (μM)	n_H (Hill coeff)	Tension Cost	N
wt	37.3 ± 1.6	2.4 ± 0.3	4.4 ± 0.7	388.5 ± 25.2	2.2 ± 0.2	3.1 ± 0.4	8.6 ± 0.5	12 (8);
wt-P	30.1 ± 0.8^b	5.2 ± 0.4^b	3.6 ± 0.5	235.2 ± 16.2^b	6.0 ± 0.8^b	1.9 ± 0.5^b	5.7 ± 0.5^b	10 (8);
del	28.2 ± 1.6^b	1.5 ± 0.1^b	4.9 ± 0.5	299.2 ± 22.2^b	1.4 ± 0.1^b	3.5 ± 0.4	8.9 ± 0.9	11 (9);
del-P	$10.7 \pm 1.4^{b,c}$	1.6 ± 0.1^b	4.1 ± 0.3	$222.4 \pm 28.0^{b,c}$	1.5 ± 0.6^b	2.6 ± 0.4	$17.9 \pm 0.6^{b,c}$	9 (7);

[a] Fiber bundles in which the endogenous Tn complexes were exchanged with recombinant Tn complexes, containing TnI-wt, TnC-wt, and various TnT's, were used to simultaneously measure changes in Ca^{2+} dependence of isometric tension and ATPase activity. Tension cost is defined as the slope of the relation between ATPase activity and isometric tension. N represents the number of fibers (hearts) used for each group. [b] $p < 0.05$ as compared with wild-type exchange. [c] $p < 0.05$ as compared with del exchange.

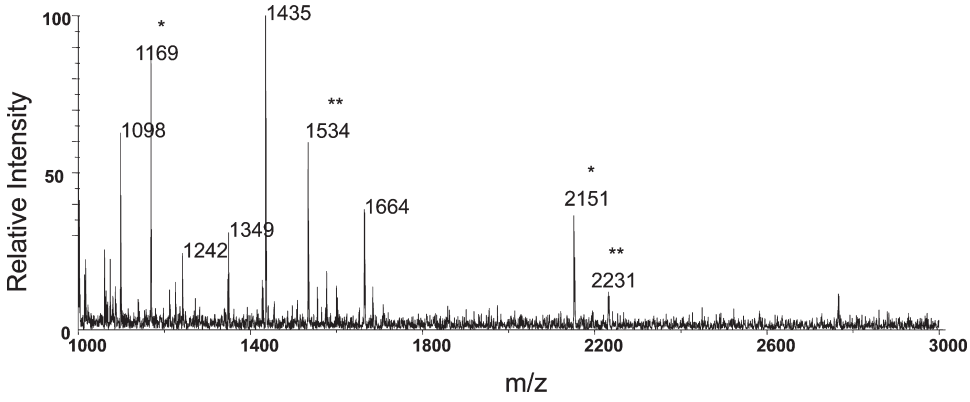

FIGURE 3: Analysis of PKC-α-phosphorylated cTnT-wt by positive ion MALDI-TOF. PKC-α-phosphorylated cTnT-wt was digested with endoproteinase Glu-C from *S. aureus* V8. Phosphopeptides were enriched by IMAC-Ga(III). Peptides with m/z 1169, 1534, 2151, and 2231 correspond to cTnT fragments: residues 202−209 (GKRQTERE) + 1 PO_4, residues 199−209 (RKSGKRQTERE) + 2 PO_4, residues 274−291 (NQKVSKTRGKAKVTGRWK) + 1 PO_4, and residues 274−291 (NQKVSKTRGKAKVTGRWK) + 2 PO_4, respectively. Asterisks indicate the presence of one or two phosphate groups.

region detach from the thin filaments; i.e., the faster they detach, the more rapidly the muscle will shorten (*32*). Cross-bridge detachment rate is determined by how fast the filaments are sliding and enter the negative force state, the rate of product release (MgADP) from the attached cross-bridge, and the rate at which ATP binds to and detaches the attached cross-bridge. Unloaded shortening velocity is not as sensitive to changes in calcium concentration as isometric force (*5*, *33*−*35*). Thus reductions in free calcium concentration that produce a fall in isometric force to about 50% of maximal have little effect on the unloaded shortening velocity (or thin filament sliding speed). Consequently, pCa_{50} for sliding speed is left-shifted with respect to that of isometric force (*35*). Further, it is has been found (particularly using TnT HCM mutations) that the maximal isometric force may fall (I79N and del160E) while the unloaded sliding speed increases markedly over controls (*36*).

Materials. Triton X-100 ampules were purchased from Pierce. Ammonium sulfate (enzyme grade) and TFA were from Fisher. 1-Palmitoyl-2-oleoyl-*sn*-glycero-3-phosphoserine (phosphatidylserine) and 1,2-*sn*-dioleoylglycerol (diacylglycerol) were purchased from Avanti Polar Lipids, Inc. All the other chemicals were from Sigma.

Animal Care. All animals were handled in accordance with the guidelines of the Animal Care Committees of our respective universities.

Data Analysis and Statistical Evaluation. Isometric tension−Ca^{2+}, ATPase−Ca^{2+}, and thin filament sliding speed−pCa relationships were fit by a nonlinear fit procedure to the modified Hill equation (KaleidaGraph Software or SigmaPlot 9) as described previously (*15*). All values are presented as mean ± SE, and values of $p < 0.05$ were the criteria of statistical significance. Statistical evaluation was by one-way ANOVA and post-hoc Dunnett's t test.

RESULTS

Chemomechanical Properties of Fiber Bundles Containing cTnT-del. Figure 1 shows a schematic representation of a longitudinal view of the major thin filament proteins emphasizing the location of three critical regions of cTnT investigated in the present study (exons 9, 13, and 16) that are "hot spots" for cardiomyopathy causing mutations and phosphorylations (*10*, *11*, *15*, *17*). The fact that some of the most lethal cardiomyopathy mutations are condensed in these "hot spots" underscores the functionally critical nature of these regions. To understand better the regulatory role of the N-terminal region of a phosphorylated cTnT, we created a truncated form of cTnT that lacks its N-terminal 91 amino acids (referred to as cTnT-del). We assessed the chemomechanical profiles of mouse left ventricular papillary muscle fiber bundles where the native cTnT was exchanged with either recombinant cTnT-wt or cTnT-del. Adult mouse recombinant cTnTs (wt or del) were expressed in *Escherichia coli* and purified to near homogeneity (see Experimental Procedures). The recombinant cTnT (wt or del) was then used to reconstitute cardiac troponin complexes in the presence of equimolar amounts of cTnI and cTnC. The heterotrimeric troponin complexes, cTn-del and cTn-wt, were then added to the respective detergent-treated (permeabilized) papillary fiber bundles to replace (exchange) the native cTn

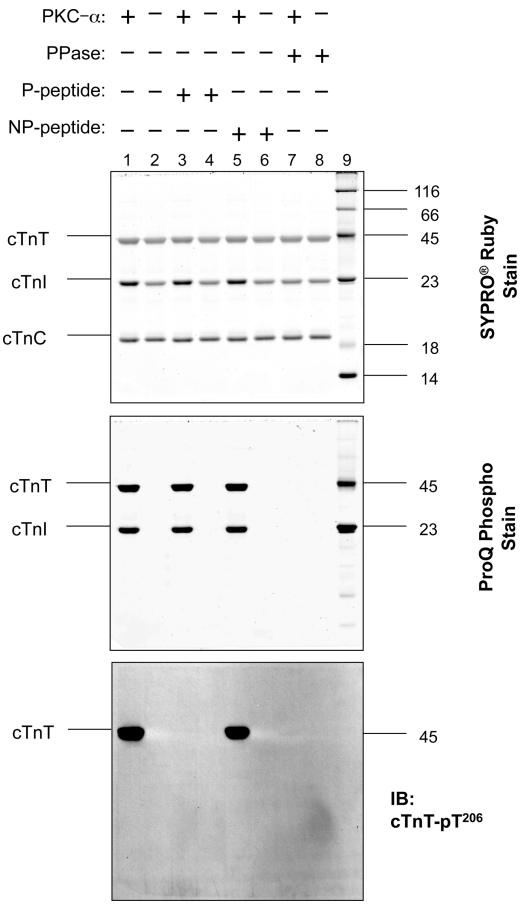

FIGURE 4: Peptide competition assay demonstrating the specificity of the anti-pT^{206} antibody. Recombinant cTn-wt complexes were resolved by SDS−PAGE on a 15% polyacrylamide gel and either stained with SYPRO Ruby total protein gel stain (top) or ProQ Diamond phosphoprotein gel stain (middle) or transferred to a PVDF membrane (bottom). cTn-wt samples resolved by SDS−PAGE were either phosphorylated by recombinant PKC-α (lanes 1, 3, 5, 7; see Experimental Procedures), left untreated (lanes 2, 4, 6, 8), or were treated with λ-PPase (lanes 7, 8; Upstate). Phosphoprotein molecular mass standards (PeppermintStick; Molecular Probes) in lane 9 contain a mixture of two phosphorylated and four nonphosphorylated proteins. The molecular masses, ranging from 14 to 116 kDa, are indicated on the right. PVDF membrane strips corresponding to each of the above lanes (cut after Ponceau Red membrane stain) were incubated with anti-pT^{206} antibody aliquots that were premixed with no peptide (lanes 1, 2, 7, 8), the phosphopeptide immunogen (lanes 3, 4), or the nonphosphopeptide corresponding to the immunogen (lanes 5, 6).

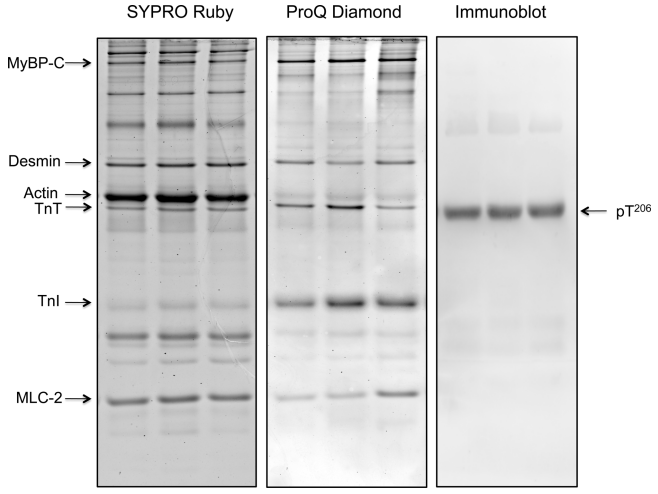

FIGURE 5: Anti-pThr^{206} antibody does not cross-react with other phosphorylated sarcomeric proteins. Myofilament proteins from isolated murine cardiac myofibrils (*45*) were resolved by 15% SDS−PAGE (left lane, C57Bl/6 male; middle lane, FVBN male; right lane, FVBN female). The left panel shows Sypro Ruby total protein stain. Major sarcomeric proteins are labeled. The middle panel shows the basal phosphorylation state of myofilaments as detected by ProQ Diamond. The right panel depicts the specific reactivity of anti-pThr206 antibody.

complex. This gentle exchange procedure allows for a gradual replacement of native cTn by cTn-del (or cTn-wt) with no major alteration to the fiber properties, since the myofilaments are never depleted of cTn (*15*, *26*−*28*).

Figure 2 illustrates results from (A) tension development (i.e., force divided by cross-sectional area of the fiber bundles), (B) actomyosin Mg-ATPase rate (determined simultaneously with force), and (C) tension cost (the slope of the ATP consumption−tension relationship, also serving as an index of cross-bridge cycling) at various [Ca^{2+}]. Table 1 summarizes the mechanical and energetic profiles of fiber experiments. Incorporation of cTnT-del into the myofibrillar matrix leads to a reduction of maximal tension (by 24%) and actomyosin-ATPase activity (by 23%). This effect is associated with a leftward shift in Ca^{2+} sensitivity (EC_{50}, i.e., [Ca^{2+}] at which force is half-maximal of 1.5 ± 0.1 compared with 2.4 ± 0.3 μM for cTn-wt) with no change in cooperativity of thin filament activation, as indexed by n_H, the Hill coefficient (n_H of 4.9 ± 0.5 compared to 4.4 ± 0.7 for cTn-wt). At EC_{50} cTn-del fibers generate 57% more tension and have 48% higher ATPase activity than that of cTn-wt fibers. Therefore, removal of the 91 amino acid N-terminal tail of cTnT increases the sensitivity of the contractile apparatus to Ca^{2+}, suggesting an important role in myofilament activation.

Analysis of Site-Specific Phosphorylation of cTnT Constructs. Cardiac TnT is phosphorylated in the human and rodent hearts even under basal conditions (Garcia-Cazarin and Sumandea, unpublished observation). However, until now, studies aimed at investigating the role of the N-terminal region have not considered the effects of phosphorylation (*12*−*14*). Our work with several recombinant PKCs (α, βII, δ, and ε) identified PKC-α as being most efficient in phosphorylating recombinant cTnT *in vitro*. The other PKCs (βII, δ, and ε) while able to phosphorylate cTnT (as well as cTnI) as part of the troponin complex have a lower preference for cTnT alone (data not shown). To investigate the role of cTnT phosphorylation in the absence of confounding cTnI phosphorylation events, we used PKC-α to efficiently phosphorylate cTnT prior to incorporation in the troponin complex. Therefore, cTnT-del and cTnT-wt were phosphorylated by PKC-α, in preparation for complex reconstitution and exchange experiments.

Mass spectrometric analysis was used to identify the specific cTnT sites phosphorylated in a PKC-α-dependent manner (Figure 3). We employed both isolated cTnT (wt and del) and troponin complexes (wt and del). Our data indicate that PKC-α phosphorylates cTnT-wt at four sites: Ser^{201}, Thr^{206}, Ser^{278}, and Thr^{287} (mouse sequence; Figure 1). The same sites were identified in samples containing phosphorylated cTnT-del and cTnTs from cTn complexes (data not shown). Thr^{206} was the major phosphorylation site *in vitro*. Previous work from our laboratory identified Thr^{206} as the functionally critical PKC phosphorylation residue, while the other sites do not seem to have an obvious functional role (*15*). Three of these sites Ser^{201}, Thr^{206}, and Thr^{287}, were previously reported as PKC phosphorylation

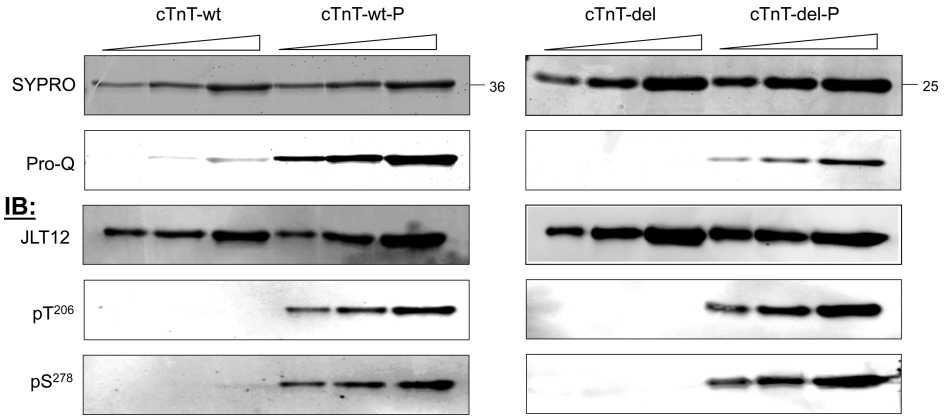

FIGURE 6: PKC-α-dependent phosphorylation of cTnT-wt and cTnT-del. Recombinant mouse cTnT-wt (0.5, 1.0, 2.0 μg) and cTnT-del (0.5, 1.0, 2.0 μg) prepared for exchange experiments (phosphorylated and nonphosphorylated) were resolved by SDS−PAGE on a 15% polyacrylamide gel and either stained with SYPRO Ruby total protein gel stain or ProQ Diamond phosphoprotein gel stain or transferred to a PVDF membrane and immunoblotted with anti-pan cTnT (JLT12, Sigma), anti-phospho-specific pThr^{206}, or pSer^{278} antibodies.

sites (*16*). Ser^{278} was shown recently to be a ROCK substrate (*18*). The present study also assigns cTnT-Ser^{278} kinase activity to PKC-α.

The need to monitor and quantify phosphorylation of cTnT at the functionally significant site, Thr^{206}, led us to develop phosphorylation site-specific antibodies that react only with phosphorylated Thr^{206}. Figure 4 illustrates a peptide competition assay that demonstrates the phospho specificity of anti-pThr^{206} antibody. The top panel shows a representative gel stained with the Sypro Ruby total protein stain, demonstrating equal loading of samples. The middle panel shows the same gel (above) this time stained with ProQ Diamond phosphostain, identifying the presence of phosphoproteins (for details, see Experimental Procedures). As expected, both cTnI and cTnT were phosphorylated by PKC-α but not cTnC. PKC-phosphorylated samples that were treated with λ phosphatase (λPPase, lanes 7, 8), to remove all phosphate groups, are not detected with ProQ Diamond, indicating complete dephosphorylation. The bottom panel shows immunoblot detection using anti-pThr^{206} antibody. While ProQ Diamond detects cTnT and cTnI phosphorylation (lane 1), anti-pT^{206} antibody reacts only with phosphorylated cTnT. Nonphosphorylated cTnT and cTnI (lane 2) are only detected by the Sypro Ruby stain. Lanes 3 and 4 contain PKC-phosphorylated and nonphosphorylated cTn (respectively). For the immunoblot, the pThr^{206} antibody was preincubated for 30 min with the phosphopeptide immunogen. The phosphopeptide competes for the antibody's recognition site and abolishes its reactivity with the phosphorylated Thr^{206} residue (indicative of the antibody's specificity for phospho-Thr^{206}). The antibody's specificity is further proved by the fact that the nonphosphopeptide (lanes 5, 6), which does not compete for the antibody's recognition site, had not affected its ability to detect phosphorylated Thr^{206}. It is worth mentioning that the anti-pThr^{206} antibody does not recognize dephosphorylated TnT (lanes 7, 8).

Additionally, the anti-pThr^{206} reactivity was tested in isolated cardiac myofibrils from three different 5−6 month-old mouse hearts (C57Bl/6 male, FVBN male, and FVBN female). Myofibrillar proteins were resolved by 15% SDS−PAGE and then stained for total protein content by Sypro Ruby, total phosphorylation levels by ProQ Diamond, and pThr^{206} phosphorylation by immunoblotting with anti-pThr^{206} antibody (Figure 5). Data indicate that anti-pThr^{206} antibody is site specific and has no reactivity with other phosphorylated sarcomeric proteins.

Next, cTnT-pThr^{206} and -pSer^{278} (control) antibodies were used to analyze troponin complexes prepared for fiber exchange or *in vitro* motility experiments (harboring cTnT-wt-P and cTnT-del-P). Figure 6 shows cTnT samples probed with Sypro Ruby for total protein and ProQ Diamond for phosphoprotein content or immunoblotted with anti-cTnT antibodies as indicated. Our data indicate similar levels of phosphorylation of both Thr^{206} and Ser^{278} (control) in samples prepared for fiber exchange or *in vitro* motility assays.

Effects of PKC-Dependent Phosphorylation of cTnT-del on Myofilament Function. Figure 7 and Table 1 summarize cTnT phosphorylation data. These data validate our previous observation (*15*) that cTnT-wt phosphorylation by PKC-α (i.e., cTn-wt-P) significantly reduces the maximal force-generating capacity of the myofilaments (by 20%), concomitant with a depression in ATPase activity (by 40%) and desensitization to calcium, as compared with cTn-wt fibers. Interestingly, cTn-wt-P fibers exhibit a decrease in tension cost compared with cTn-wt fibers (Figures 7C and 8C), indicating reduced cross-bridge cycling.

A striking aspect of data in Figure 7 is that cTn-del-P fibers severely depress the tension development of the myofilaments (by 70%) at maximal [Ca^{2+}] compared with cTn-wt fibers. Additionally, the ATPase activity rate falls by 42% in cTn-del-P fibers. This change is associated with a leftward shift in Ca^{2+} sensitivity compared with cTn-wt. While phosphorylation of cTnT-wt decreases tension cost, absence of the N-terminal tail of phosphorylated cTnT (i.e., cTn-del-P) increases it (Table 1, Figures 7C and 8C).

In Vitro Motility Assay Measurements. To further evaluate the functional effects of phosphorylation and cleavage of the cTnT N-terminus tail, we used the *in vitro* motility assay to measure reconstituted thin filaments sliding speed over myosin heads at various [Ca^{2+}]. The *in vitro* motility assay is an appropriate correlate of the unloaded shortening velocity of muscle fibers (*37*, *38*). The sliding speed of thin filaments regulated by cTnT-del is more sensitive to Ca^{2+} compared with cTn-wt (Figure 9A and Table 2), like the isometric fiber data. Furthermore, we observed an increase in sliding speed at every [Ca^{2+}] in cTn-del compared with cTn-wt regulated actin filaments. The sliding speed of cTn-del at maximal [Ca^{2+}] activating (V_{max}) increases by 10%, whereas at EC_{50} increases by 50%, compared with cTn-wt regulated filaments. Phosphorylation of

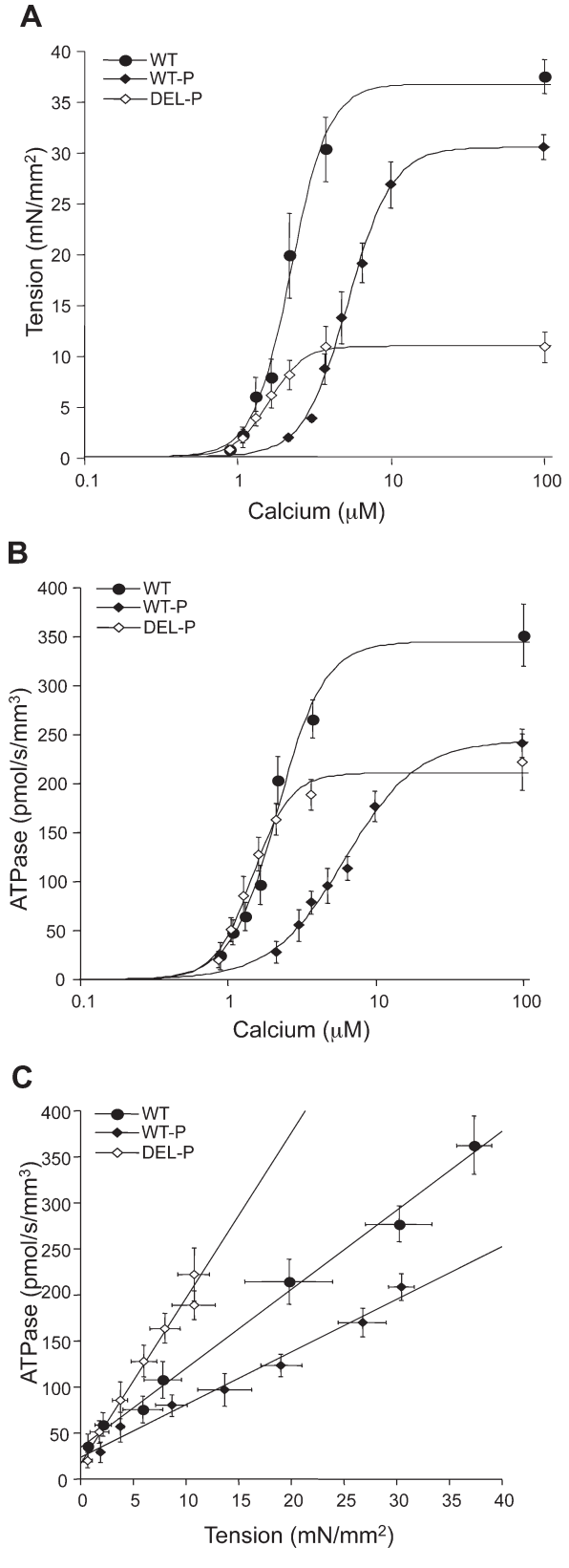

FIGURE 7: Mechanical characteristics of skinned fiber bundles in which native cTn complexes were exchanged with recombinant cTn-wt, cTn-wt-P, or cTn-del-P. P indicates PKC-α-phosphorylated cTnT. Steady-state isometric tension (A) and actomyosin Mg-ATPase activity (B) were determined simultaneously at various [Ca^{2+}]. Tension cost (C) was determined from the slope of the relationship between actomyosin Mg-ATPase activity and isometric tension. Data are given as means ± SEM for $n = 8$ fiber bundles from eight separate hearts.

cTnT (whether cTnT-del or -wt) markedly depresses sliding speed at all [Ca^{2+}] (Figure 9 and Table 2). This change is also associated with a Ca^{2+} desensitization of sliding filaments. Additionally, phosphorylation of cTnT (whether cTnT-del or -wt) also alters the cooperativity of thin filament activation compared with nonphosphorylated cTnT-wt (Table 2).

DISCUSSION

Data presented here are the first to report the specific role of the N-terminal tail of cTnT in the presence of phosphorylation on chemomechanical properties of cardiac myofilaments. The important and novel findings of our study are that (i) the incorporation of cTnT-del in the cardiac sarcomere results in decreased maximal Ca^{2+}-activated force and increased myofilament Ca^{2+} sensitivity and (ii) phosphorylation of cTnT-del leads to a severe fall of force concomitant with an increase in tension cost indicating augmentation of cross-bridge cycling (detachment) rates. Interestingly, incorporation of the intact phosphorylated cTnT (cTnT-wt-P) in the myofilament lattice decreases myofilament force (albeit more moderately compared with cTnT-del-P), significantly desensitizes myofilaments to Ca^{2+}, and lowers cross-bridge cycling rates (as indexed by the tension cost). In agreement with fiber data, the sliding speed of thin filaments regulated by cTn-del is more sensitive to Ca^{2+} compared with cTn-wt. Phosphorylation of cTnT (whether cTnT-del or -wt) markedly depresses sliding speed and is associated with Ca^{2+} desensitization of thin filaments. These data are consistent with a molecular model of Ca^{2+}-dependent cardiac muscle activation in which the N-terminal region of cTnT has an inhibitory effect on myosin interaction with thin filaments, probably through stabilization of Tm-actin conformation in a blocked state. Removal of the cTnT N-terminal fragment 1−91 relieves this inhibitory effect. We propose that cTnT phosphorylation alters cTnT/cTnI interaction and impairs the transduction of Ca^{2+} signaling to Tm.

Results of the present study are consistent with earlier findings examining the role of the N-terminal domain of cTnT and extend them to include the functional effect of phosphorylation. Biesiadecki et al. (*12*) deleted the N-terminal hypervariable region of mouse cTnT (amino acids 1−71) and observed that the truncated protein retained similar binding affinities to cTnI and Tm as the intact cTnT. The authors suggested that the polypeptide (amino acids 72−291) forms the core structure responsible for protein binding activities of cTnT. Interestingly, removal of amino acids 1−91, resulting in a similar fragment as the one used in this study, diminished the binding affinity to Tm. Their data extend an earlier study by Pan et al. (*14*) that showed the first 45 N-terminal residues of rabbit skeletal TnT are not essential for anchoring the troponin complex to the thin filament. Using a myofibrillar MgATPase assay, Chandra et al. (*13*) demonstrated that elimination of amino acids 1−76 from rat cardiac TnT depressed the ATPase activity by 30% at maximal [Ca^{2+}], with no change in myofilament sensitivity to Ca^{2+}. Deletion of amino acids 1−91 from mouse cTnT leads to a 23% drop in maximal MgATPase activity and a significant sensitization of exchanged skinned fibers. Enhanced thin filament Ca^{2+} sensitivity observed in our study (not observed in ref *13*) apparently arose from removal of cTnT fragment 77−91, which seems to contain essential residues responsible for binding to Tm (*12*).

Single cardiomyopathy-causing mutations localized in the vicinity of amino acid 91 (truncation site) are also known to increase myofilament Ca^{2+} sensitivity (*10*, *11*, *39*). Further support for the importance of this region ("hot spot 1") in

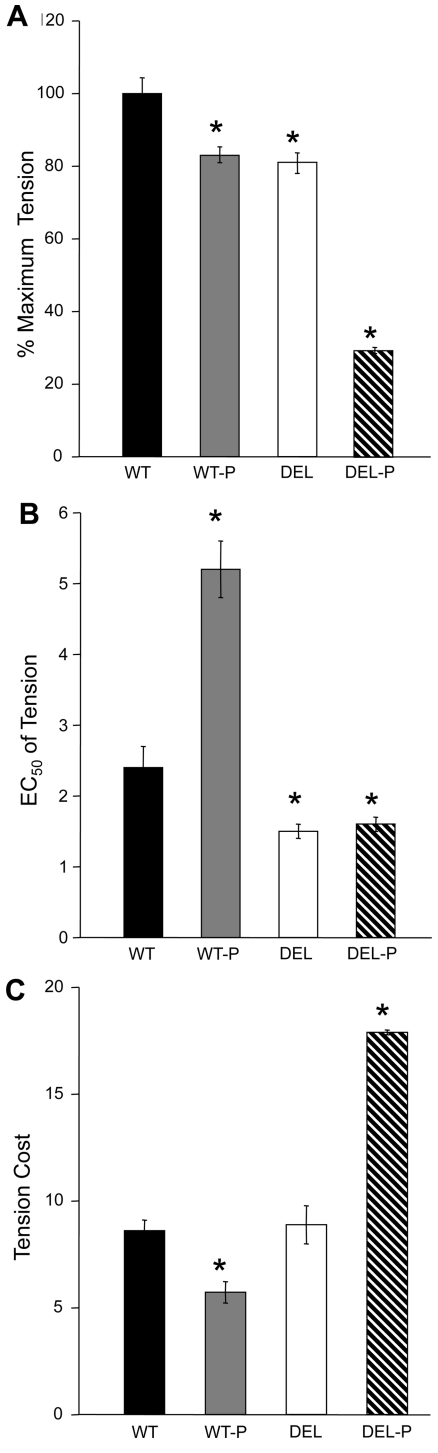

FIGURE 8: Summary of Ca^{2+} sensitivity and mechanical characteristics of skinned fibers exchanged with cTn-wt, cTn-wt-P, cTn-del, and cTn-del-P. (A) Summary of maximum tension measurements normalized to the maximum tension determined in fibers exchanged with cTn-wt. Compared with cTn-wt, the decrease in maximum tension was significantly lower in all of the fibers containing modified cTnT's (wt-P, del, del-P). (B) Summary of $[Ca^{2+}]$ at 50% maximum tension; EC_{50} represents the myofilament calcium sensitivity index. Fibers containing cTnT-wt-P show a dramatic increase with EC_{50} indicating desensitization to Ca^{2+} (i.e., it takes more $[Ca^{2+}]$ to reach 50% maximum tension). On the other hand, fibers containing cTnT-del are more sensitive to Ca^{2+} compared to cTnT-wt. (C) Summary of tension cost, an index of cross-bridge cycling rate. Compared with wt, cTnT-wt-P decreases whereas cTnT-del-P increases myofilament tension cost. Asterisks indicate values of $p < 0.05$.

modulating the threshold for Ca^{2+} activation comes from Palm et al. (*40*). The authors showed that mutations of residues in "hot spot 1", such as R92L, R92Q, R92W, and R94L, impair Tm-dependent functions of TnT by weakening its binding to Tm. These mutants have a lesser ability to stabilize the Tm overlap region and Tm binding to actin. Tobacman et al. (*7*) and Maytum et al. (*8*) independently concluded that the cardiac troponin T N-terminal tail has intrinsic cross-bridge inhibitory properties. These data are in agreement with our model that removal of N-terminal segment 1−91 lowers the affinity of cTnT to Tm and leads to a more flexible Tm-Tm end-to-end interaction and a myofilament disinhibition state that facilitates strong cross-bridge formation at lower activating $[Ca^{2+}]$ (Figure 9B). However, this scenario is different at saturating $[Ca^{2+}]$ where an intact N-terminal tail seems to be indispensable for maximal activation of myofilaments.

Previous studies investigating the role of the N-terminal region of cTnT in myofilament activation have not examined the role of phosphorylation. Noland et al. (*41*) using 2-D phosphopeptide mapping and sequence analysis identified residues Thr^{197}, Ser^{201}, Thr^{206}, and Thr^{287} as cTnT phosphorylation sites. Our systematic analysis of the functional role of each of these phosphorylation sites identified a distinct region of cTnT centered on Thr^{206} that when modified by phosphorylation controls force, ATPase rate, cooperativity, Ca^{2+} sensitivity, and tension cost of fiber bundles (*15*). We concluded that Thr^{206} was the functionally critical phosphorylation residue and phosphorylation of the other sites had no apparent functional effect (although they probably enhance the effect of Thr^{206} phosphorylation). In the present study, mass spectrometry analysis of PKC-α-phosphorylated cTnT identified three known phosphorylation sites, Ser^{201}, Thr^{206}, Thr^{287}, and a novel PKC-α-dependent cTnT phosphorylation site at Ser^{278}. Vahebi et al. (*18*) demonstrated earlier that Rho-A-dependent kinase II (ROCK-II) phosphorylates cTnT at Ser^{278} and Thr^{287}. Our present study, using phospho-specific antibodies, indicates that both Thr^{206} and Ser^{278} (control) were phosphorylated to a similar extent by PKC-α in both cTnT-wt and -del.

Insufficient information exists describing the mechanism by which cTnT phosphorylation alters function. Finley et al. (*42*), using NMR and small-angle X-ray scattering (SAXS), examined the consequences of cTnT-Thr^{206} phosphorylation on the dynamic properties of the troponin complex. Chemical shift mapping (CSM) and hydrogen−deuterium exchange (HDE) showed that modification of Thr^{206} (in this case by substitution to glutamic acid (E) to mimic phosphorylation) induced no significant cTnC conformational perturbations. However, SAXS analyses showed an ~18% decrease in the radius of gyration for the cTn-T206E trimeric complex compared with cTn-wt. These data suggest a compaction of the whole troponin complex as a result of a single amino acid modification in cTnT (mimicking phosphorylation). Computational analyses using the helical content prediction algorithm AGADIR (*15*) suggest that introduction of negative charges at amino acid 206 (by E substitution) extends the 206−225 α-helix by five amino acids to 200−225. The extension could potentially lead to a three-helical bundle packing of the core regions of cTnT/cTnI. On the basis of our data and the above reports, we propose that phosphorylation of cTnT at the functionally significant site Thr^{206} transmits its effect to the myofilament through internal stabilization of the cTn complex, making it less efficient (more rigid) at propagating the Ca^{2+} signal.

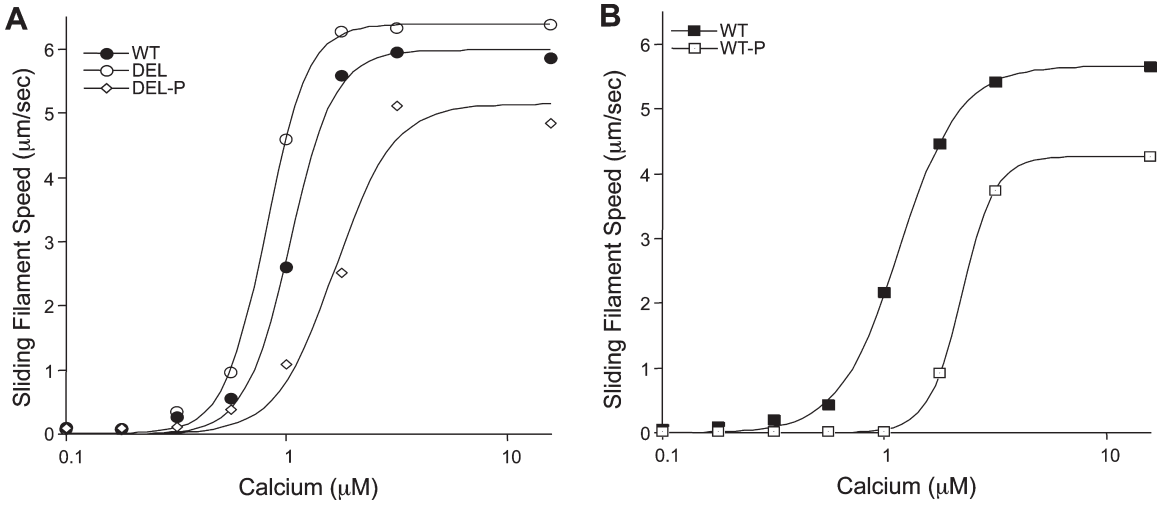

FIGURE 9: Effects of cTnT N-terminal deletion and phosphorylation on *in vitro* motility. Rhodamine phalloidin-labeled thin filaments were applied to heavy meromyosin coated surfaces, and sliding speed was monitored in the presence of ATP. Ca^{2+} affinity increased when thin filaments were regulated by cTnT-del and decreased in the presence of cTnT-del-P or cTnT-wt-P. Data points are averages of all continuously moving filaments ($n = 150-300$ for each $[Ca^{2+}]$).

Table 2: Summary of Results from *in Vitro* Motility Assay Studies[a]

	sliding speed		
TnT	V_{max} (μm/s)	EC_{50} (μM)	n_H (Hill coeff)
wt	5.9 ± 0.10	1.0 ± 0.03	4.3 ± 0.5
wt-P	4.3 ± 0.01^b	2.2 ± 0.01^b	5.6 ± 0.1^b
del	6.5 ± 0.06^b	0.8 ± 0.01^b	4.6 ± 0.3
del-P	$5.1 \pm 0.04^{b,c}$	$1.6 \pm 0.03^{b,c}$	$3.3 \pm 0.7^{b,c}$

[a] Reconstituted thin filaments regulated by various forms of TnT were examined in the *in vitro* motility assay. Tn complexes, containing TnI-wt, TnC-wt, and various TnT's (see table), were used to determine Ca^{2+} dependence of sliding filament speed. [b] $p < 0.05$ as compared with wild-type exchange. [c] $p < 0.05$ as compared with del exchange.

In an earlier comparison of the effects of calcium on unloaded shortening velocity and isometric force, Morris and Homsher (*35*) showed that the pCa_{50} (negative log of EC_{50}) for unloaded shortening was about 0.2 pCa unit greater (EC_{50} reduced by about 1.6-fold) than that for the force−pCa curve. They also showed that the Hill coefficient was 20−60% greater for the unloaded shortening velocity−pCa curve than for the force−pCa curve. The data reported above are consistent with that behavior. It is important to recognize that the unloaded shortening velocity (*in vitro* thin filament sliding speed) is largely set by the rate of ADP release from the negatively strained cross-bridges during rapid shortening (Huxley's value g_2 (*32*)) while the isometric force is proportional to $f/(f + g)$ (where f is the rate of cross-bridge attachment and g is the rate of cross-bridge detachment during isometric contractions) (*30*). Brenner (*30*) has also shown that the ATPase rate during isometric contraction is proportional to $f/(f+g)$. Thus the tension cost will be proportional to $[fg/(f+g)]/[f/(f+g)] = g$. The reduced tension cost for the cTnT-wt-P fibers is consistent with the smaller reduction in isometric force ($f/(f+g)$, 20%) than thin filament sliding speed (g_2, 29%). Similarly, the increased tension cost of the cTnT-del-P fits with the large reduction in force ($f/(f+g)$, 72% drop) and relatively smaller decline in unloaded sliding speed (g_2, 15% reduction). The implication for the cardiac muscle is that the energetic cost (ATP consumption) of both pressure and volume work in the cTnT-del-P muscle will be markedly elevated (*43*).

The present study underscores the functionally important role of cTnT posttranslational modifications (proteolysis and phosphorylation) in regulation of myofilament activation. Posttranslational modifications of cTnT have the potential of fine-tuning myocardial function to match hemodynamic demands.

REFERENCES

1. VanBuren, P., and Okada, Y. (2005) Thin filament remodeling in failing myocardium. *Heart Failure Rev. 10*, 199–209.
2. Solaro, R. J. (2001) Modulation of cardiac myofilament activity by protein phosphorylation, in Handbook of Physiology Section 2: The Cardiovascular System (Berne, R. M., Ed.) pp 264−300, Oxford University Press, Oxford, U.K.
3. Metzger, J. M., and Westfall, M. V. (2004) Covalent and noncovalent modification of thin filament action: the essential role of troponin in cardiac muscle regulation. *Circ. Res. 94*, 146–158.
4. Kobayashi, T., and Solaro, R. J. (2005) Calcium, thin filaments, and the integrative biology of cardiac contractility. *Annu. Rev. Physiol. 67*, 39–67.
5. Gordon, A. M., Homsher, E., and Regnier, M. (2000) Regulation of contraction in striated muscle. *Physiol. Rev. 80*, 853–924.
6. Gordon, A. M., Regnier, M., and Homsher, E. (2001) Skeletal and cardiac muscle contractile activation: tropomyosin "rocks and rolls". *News Physiol. Sci. 16*, 49–55.
7. Tobacman, L. S., Nihli, M., Butters, C., Heller, M., Hatch, V., Craig, R., Lehman, W., and Homsher, E. (2002) The troponin tail domain promotes a conformational state of the thin filament that suppresses myosin activity. *J. Biol. Chem. 277*, 27636–27642.
8. Maytum, R., Geeves, M. A., and Lehrer, S. S. (2002) A modulatory role for the troponin T tail domain in thin filament regulation. *J. Biol. Chem. 277*, 29774–29780.
9. Marston, S. B., and Redwood, C. S. (2003) Modulation of thin filament activation by breakdown or isoform switching of thin filament proteins: physiological and pathological implications. *Circ. Res. 93*, 1170–1178.
10. Tardiff, J. C. (2005) Sarcomeric proteins and familial hypertrophic cardiomyopathy: linking mutations in structural proteins to complex cardiovascular phenotypes. *Heart Failure Rev. 10*, 237–248.
11. Morimoto, S. (2008) Sarcomeric proteins and inherited cardiomyopathies. *Cardiovasc. Res. 77*, 659–666.
12. Biesiadecki, B. J., Chong, S. M., Nosek, T. M., and Jin, J. P. (2007) Troponin T core structure and the regulatory NH_2-terminal variable region. *Biochemistry 46*, 1368–1379.
13. Chandra, M., Montgomery, D. E., Kim, J. J., and Solaro, R. J. (1999) The N-terminal region of troponin T is essential for the maximal activation of rat cardiac myofilaments. *J. Mol. Cell. Cardiol. 31*, 867–880.
14. Pan, B. S., Gordon, A. M., and Potter, J. D. (1991) Deletion of the first 45 NH2-terminal residues of rabbit skeletal troponin T strengthens

binding of troponin to immobilized tropomyosin. *J. Biol. Chem. 266*, 12432–12438.
15. Sumandea, M. P., Pyle, W. G., Kobayashi, T., de Tombe, P. P., and Solaro, R. J. (2003) Identification of a functionally critical protein kinase C phosphorylation residue of cardiac troponin T. *J. Biol. Chem. 278*, 35135–35144.
16. Jideama, N. M., Noland, T. A., Jr., Raynor, R. L., Blobe, G. C., Fabbro, D., Kazanietz, M. G., Blumberg, P. M., Hannun, Y. A., and Kuo, J. F. (1996) Phosphorylation specificities of protein kinase C isozymes for bovine cardiac troponin I and troponin T and sites within these proteins and regulation of myofilament properties. *J. Biol. Chem. 271*, 23277–23283.
17. Noland, T. A., Jr., and Kuo, J. F. (1993) Protein kinase C phosphorylation of cardiac troponin I and troponin T inhibits Ca(2+)-stimulated MgATPase activity in reconstituted actomyosin and isolated myofibrils, and decreases actin-myosin interactions. *J. Mol. Cell. Cardiol. 25*, 53–65.
18. Vahebi, S., Kobayashi, T., Warren, C. M., de Tombe, P. P., and Solaro, R. J. (2005) Functional effects of rho-kinase-dependent phosphorylation of specific sites on cardiac troponin. *Circ. Res. 96*, 740–747.
19. He, X., Liu, Y., Sharma, V., Dirksen, R. T., Waugh, R., Sheu, S. S., and Min, W. (2003) ASK1 associates with troponin T and induces troponin T phosphorylation and contractile dysfunction in cardiomyocytes. *Am. J. Pathol. 163*, 243–251.
20. Pfleiderer, P., Sumandea, M. P., Rybin, V. O., Wang, C., and Steinberg, S. F. (2009) Raf-1: a novel cardiac troponin T kinase. *J. Muscle Res. Cell Motil. 30*, 67–72.
21. Burkart, E. M., Sumandea, M. P., Kobayashi, T., Nili, M., Martin, A. F., Homsher, E., and Solaro, R. J. (2003) Phosphorylation or glutamic acid substitution at protein kinase C sites on cardiac troponin I differentially depress myofilament tension and shortening velocity. *J. Biol. Chem. 278*, 11265–11272.
22. Chandra, M., Kim, J. J., and Solaro, R. J. (1999) An improved method for exchanging troponin subunits in detergent skinned rat cardiac fiber bundles. *Biochem. Biophys. Res. Commun. 263*, 219–223.
23. Yang, X., Wu, H., Kobayashi, T., Solaro, R. J., and van Breemen, R. B. (2004) Enhanced ionization of phosphorylated peptides during MALDI TOF mass spectrometry. *Anal. Chem. 76*, 1532–1536.
24. Kobayashi, T., Yang, X., Walker, L. A., Van Breemen, R. B., and Solaro, R. J. (2005) A non-equilibrium isoelectric focusing method to determine states of phosphorylation of cardiac troponin I: identification of Ser-23 and Ser-24 as significant sites of phosphorylation by protein kinase C. *J. Mol. Cell. Cardiol. 38*, 213–218.
25. Janssen, P. M., and de Tombe, P. P. (1997) Protein kinase A does not alter unloaded velocity of sarcomere shortening in skinned rat cardiac trabeculae. *Am. J. Physiol. 273*, H2415–H2422.
26. Brenner, B., and Chalovich, J. M. (1999) Kinetics of thin filament activation probed by fluorescence of N-((2-(iodoacetoxy)ethyl)-N-methyl)amino-7-nitrobenz-2-oxa-1, 3-diazole-labeled troponin I incorporated into skinned fibers of rabbit psoas muscle: implications for regulation of muscle contraction. *Biophys. J. 77*, 2692–2708.
27. She, M., Trimble, D., Yu, L. C., and Chalovich, J. M. (2000) Factors contributing to troponin exchange in myofibrils and in solution. *J. Muscle Res. Cell Motil. 21*, 737–745.
28. Kohler, J., Chen, Y., Brenner, B., Gordon, A. M., Kraft, T., Martyn, D. A., Regnier, M., Rivera, A. J., Wang, C. K., and Chase, P. B. (2003) Familial hypertrophic cardiomyopathy mutations in troponin I (K183D, G203S, K206Q) enhance filament sliding. *Physiol. Genomics 14*, 117–128.
29. de Tombe, P. P., and Stienen, G. J. (1995) Protein kinase A does not alter economy of force maintenance in skinned rat cardiac trabeculae. *Circ. Res. 76*, 734–741.
30. Brenner, B., and Eisenberg, E. (1986) Rate of force generation in muscle: correlation with actomyosin ATPase activity in solution. *Proc. Natl. Acad. Sci. U.S.A. 83*, 3542–3546.
31. Heller, M. J., Nili, M., Homsher, E., and Tobacman, L. S. (2003) Cardiomyopathic tropomyosin mutations that increase thin filament Ca^{2+} sensitivity and tropomyosin N-domain flexibility. *J. Biol. Chem. 278*, 41742–41748.
32. Huxley, A. F. (1957) Muscle structure and theories of contraction. *Prog. Biophys. Biophys. Chem. 7*, 255–318.
33. Metzger, J. M., and Moss, R. L. (1988) Thin filament regulation of shortening velocity in rat skinned skeletal muscle: effects of osmotic compression. *J. Physiol. 398*, 165–175.
34. Moss, R. L. (1986) Effects on shortening velocity of rabbit skeletal muscle due to variations in the level of thin-filament activation. *J. Physiol. 377*, 487–505.
35. Morris, C. A., Tobacman, L. S., and Homsher, E. (2003) Thin filament activation and unloaded shortening velocity of rabbit skinned muscle fibres. *J. Physiol. 550*, 205–215.
36. Sweeney, H. L., Feng, H. S., Yang, Z., and Watkins, H. (1998) Functional analyses of troponin T mutations that cause hypertrophic cardiomyopathy: insights into disease pathogenesis and troponin function. *Proc. Natl. Acad. Sci. U.S.A. 95*, 14406–14410.
37. Homsher, E., Kim, B., Bobkova, A., and Tobacman, L. S. (1996) Calcium regulation of thin filament movement in an in vitro motility assay. *Biophys. J. 70*, 1881–1892.
38. Homsher, E., Wang, F., and Sellers, J. R. (1992) Factors affecting movement of F-actin filaments propelled by skeletal muscle heavy meromyosin. *Am. J. Physiol. 262*, C714–C723.
39. Gomes, A. V., and Potter, J. D. (2004) Molecular and cellular aspects of troponin cardiomyopathies. *Ann. N.Y. Acad. Sci. 1015*, 214–224.
40. Palm, T., Graboski, S., Hitchcock-DeGregori, S. E., and Greenfield, N. J. (2001) Disease-causing mutations in cardiac troponin T: identification of a critical tropomyosin-binding region. *Biophys. J. 81*, 2827–2837.
41. Noland, T. A., Jr., Raynor, R. L., and Kuo, J. F. (1989) Identification of sites phosphorylated in bovine cardiac troponin I and troponin T by protein kinase C and comparative substrate activity of synthetic peptides containing the phosphorylation sites. *J. Biol. Chem. 264*, 20778–20785.
42. Finley, N. L., Heller, W. T., Sumandea, M. P., Solaro, R. J., Trewhella, J., and Rosevear, P. R. (2004) Mechanisms of phosphorylation induced modulation of cardiac troponin, Biophys. J., Suppl. , Abstract, 2058-Pos.
43. Katz, A. M. (2006) Physiology of the heart , 4th ed., Lippincott Williams & Wilkins, Philadelphia, PA.
44. Takeda, S., Yamashita, A., Maeda, K., and Maeda, Y. (2003) Structure of the core domain of human cardiac troponin in the Ca(2+)-saturated form. *Nature 424*, 35–41.
45. Arteaga, G. M., Warren, C. M., Milutinovic, S., Martin, A. F., and Solaro, R. J. (2005) Specific enhancement of sarcomeric response to Ca^{2+} protects murine myocardium against ischemia-reperfusion dysfunction. *Am. J. Physiol. Heart Circ. Physiol. 289*, H2183–H2192.